



**HAL**  
open science

## New hydrophobic deep eutectic solvent for electrochemical applications

Nesrine Chaabene, Kieu Ngo, Mireille Turmine, Vincent Vivier

► **To cite this version:**

Nesrine Chaabene, Kieu Ngo, Mireille Turmine, Vincent Vivier. New hydrophobic deep eutectic solvent for electrochemical applications. *Journal of Molecular Liquids*, 2020, 319, pp.114198. 10.1016/j.molliq.2020.114198 . hal-02936182

**HAL Id: hal-02936182**

**<https://hal.sorbonne-universite.fr/hal-02936182v1>**

Submitted on 11 Sep 2020

**HAL** is a multi-disciplinary open access archive for the deposit and dissemination of scientific research documents, whether they are published or not. The documents may come from teaching and research institutions in France or abroad, or from public or private research centers.

L'archive ouverte pluridisciplinaire **HAL**, est destinée au dépôt et à la diffusion de documents scientifiques de niveau recherche, publiés ou non, émanant des établissements d'enseignement et de recherche français ou étrangers, des laboratoires publics ou privés.

# NEW HYDROPHOBIC DEEP EUTECTIC SOLVENT FOR ELECTROCHEMICAL APPLICATIONS

NESRINE CHAABENE, KIEU NGO, MIREILLE TURMINE, VINCENT VIVIER

Sorbonne Université, CNRS, Laboratoire Interfaces et Systèmes Electrochimiques, LISE,

F-75005 Paris, France

## Abstract

Deep eutectic solvents (DESs) are known as cheap and biodegradable solvents which are easier to synthesize than ionic liquids (ILs). In this work, a new hydrophobic DES based on menthol is described. It consisted in a mixture of menthol and acetic acid in which ethanolamine has been added in order to increase the conductivity up to few  $\text{mS}\cdot\text{cm}^{-1}$ . The physicochemical properties as a function of temperature, in the range of 293 to 333 K, of this menthol-based DES have been compared to the ethaline, which is one of the most widely used DES. Cyclic voltammetry has been used to study the electrochemical behavior of an electroactive mediator, the hydroxymethylferrocene (FcMeOH), which is a reversible electrochemical system and its diffusion coefficient, determined in both DESs, is of the same order of magnitude than the one reported for the 1-ethyl-3-methylimidazolium bis(trifluoro-methanesulfonyl)imide (EMIMTFSI), which is the most widely used IL for electrochemical applications. This new class of DES thus provide an eco-friendly alternative for electrochemical applications.

**Keywords:** *menthol-based DES; hydrophobic solvent; biodegradable solvent; cyclic voltammetry*

Corresponding author:

Mireille Turmine: mireille.turmine@sorbonne-universite.fr

## 29        **1. Introduction**

30        With the emergence of green chemistry, ionic liquids (ILs) are currently used as an attractive  
31        alternative to organic solvents [1, 2]. Despite their many interesting physicochemical properties  
32        such as a low melting temperature ( $< 100\text{ }^{\circ}\text{C}$ ), a high thermal stability, a low vapor pressure, a  
33        non-flammability and a wide electrochemical potential window, ILs remain expensive and their  
34        preparation can be relatively complex [3, 4]. Recently, deep eutectic solvents (DESs) have been  
35        used as analogues and alternative green solvents to replace traditional solvents but also to take  
36        advantage of some of the most prominent properties of ILs [5, 6]. They are generally composed  
37        of at least two compounds bonded together by intermolecular forces such as hydrogen bonding.  
38        These interactions result in a significant decrease in the melting point of the mixture, DESs  
39        often becoming liquid at room temperature. Additionally, DESs have many advantages. For  
40        example, they can be easily synthesized with a high purity at low cost, and their components  
41        are biodegradable and have a low toxicity [7].

42        The first DESs described in the literature [8] are based on choline chloride and urea or ethylene  
43        glycol, known as reline or ethaline, respectively. Even if choline chloride is one of the most  
44        widespread components used for DESs [9-11], the presence of chloride may be a limiting factor  
45        for applications in electrochemistry. Moreover, most of these choline-based DES media suffer  
46        from their hydrophilicity. Interestingly, the almost unlimited number of possible combinations  
47        offers an infinite range of DESs that can be custom-synthesized depending on the targeted  
48        application [12] and it should also be mentioned that some DESs can be obtained by the mixing  
49        of both ionic and non-ionic species.

50        Recently, the group of Marrucho [13, 14] has reported a new hydrophobic DES prepared from  
51        menthol and an organic acid, which is used for the extraction of different biomolecules such as  
52        caffeine, tryptophan, isophthalic acid, and vanillin from the aqueous phase to the eutectic  
53        mixture phase. This new family of DESs should thus offer new perspectives for electrochemical  
54        applications, but unfortunately these DESs have a poor ionic conductivity.

55        The main objective of this work is to investigate the preparation of a new DES based on the  
56        mixture of menthol and carboxylic acid in which an amine has been added in order to increase  
57        the conductivity up to few  $\text{mS}\cdot\text{cm}^{-1}$ , while still keeping the environmentally-friendly and bio-  
58        compatible characters of the end solvent. Such a new hydrophobic DES should thus be a good  
59        candidate as a new electrolyte for electrochemical applications.

60 First, the physicochemical properties of this DES including density, viscosity, conductivity and  
61 electrochemical windows have been studied and compared to a usual DES (*i.e.* ethaline) and  
62 common hydrophobic ionic liquid (*i.e.* EMIMTFSI). Then, its use as solvent for  
63 electrochemical application has been investigated by cyclic voltammetry in presence of an  
64 electroactive probe, namely the hydroxymethylferrocene (FcMeOH).

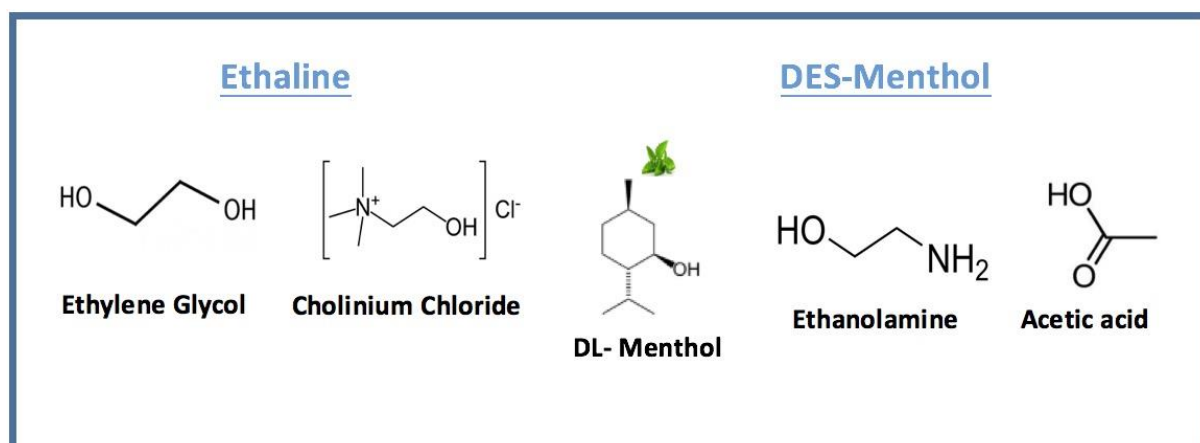
65

## 66 2. Experimental section

### 67 2.1 Chemicals and synthesis of DESs

68 Choline chloride (ChCl) (Acros Organics, purity  $\geq 99\%$ ), ethylene glycol (EG) (VWR  
69 Chemical, purity  $\geq 99\%$ ), DL-Menthol (Sigma Aldrich, purity  $\geq 95\%$ ), ethanolamine (Sigma  
70 Aldrich, purity  $\geq 98\%$ ) and acetic acid (Sigma Aldrich, purity  $\geq 99.7\%$ ) were used as received.  
71 The chemical structures of the compounds used for the synthesis of DESs are presented in Fig.  
72 1.

73



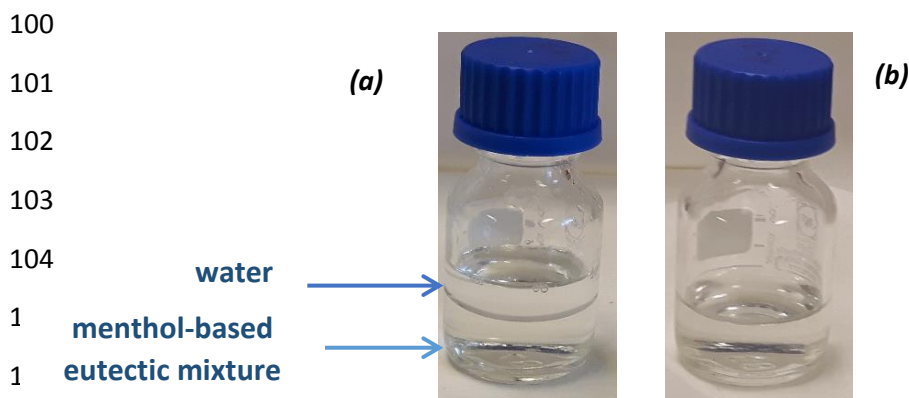
74

75 **Figure 1.** Chemical structures of the compounds used for the preparation of deep eutectic solvents  
76 studied in this work.

77

78 1-ethyl-3-methylimidazolium bis(trifluoromethanesulfonyl)imide (EMIMTFSI) was  
79 synthesized according to the method previously described in the literature [15]. Its structure  
80 was checked by <sup>1</sup>H NMR spectroscopy and ElectroSpray mass spectroscopy. <sup>1</sup>H NMR  
81 spectroscopy (400 MHz, CDCl<sub>3</sub>,  $\delta$ /ppm relative to TMS),  $\delta$  = 8.60 (s, 1H), 7.41(d, 2H,  $J=10.3$ ),  
82 4.25 (q, 2H,  $J=7.36$ ), 3.93(s, 3H), 1.54(t, 3H,  $J=7.4$ ). ElectroSpray mass spectroscopy (ESI  
83 positive):  $m/z$  = 111.1 (EMIM<sup>+</sup>); (ESI negative)  $m/z$  = 280.1 (TFSI<sup>-</sup>). The estimated purity is  
84 about 99%.

85 Ethaline was prepared by mixing cholinium chloride with ethylene glycol with a 1:2 molar  
86 ratio. The mixture was stirred for 3 hours at room temperature to yield a homogeneous and  
87 transparent liquid. The menthol-based eutectic mixture was prepared by mixing menthol,  
88 ethanolamine and acetic acid in a 1:2:4 molar ratio. The mixture of these three compounds was  
89 then heated at 80 °C for 30 min and then slowly cooled down until reaching room temperature  
90 leading to a homogeneous transparent liquid. The water content in the three freshly prepared  
91 solvent was titrated using a Karl – Fisher coulometer (C20, Mettler Toledo). Thus, the water  
92 content of the hydrophobic ionic liquid (EMIMTFSI) was 50 ppm, that of menthol-based DES  
93 was 85 ppm while the amount of water in ethaline was about 2000 ppm.  
94 The hydrophobicity test was performed in order to characterize the role of menthol (Fig. 2) by  
95 comparing two mixtures. The first one was a mixture of ethanolamine and acetic acid in a 2:4  
96 molar ratio. The second mixture was the as-prepared menthol-based eutectic solvent. The same  
97 amount of water (5 mL) was mixed with both mixtures, which resulted in the formation of two  
98 phases in the case of the menthol-based eutectic mixture (Fig. 2a), whereas the acetic acid –  
99 ethanolamine mixture mixed up with water (Fig. 2b).



108 **Figure 2:** *Hydrophobicity test for menthol-based eutectic solvent (a), and acetic acid – ethanolamine*  
109 *mixture (b)*

## 112 2.2 Physicochemical characterization of the solvents

113 The density, viscosity and ionic conductivity of all the solvents were measured using the devices  
114 listed in Table 1, in which the estimation of the average uncertainty for each physicochemical  
115 property is also reported.

118

119

**Table 1.** *Device and uncertainty for physical-chemical property measurements*

Physicochemical property	Measurement device	Standard uncertainty
Density	Anton Paar DMA 5000	Less than 0.05 kg m <sup>-3</sup>
Viscosity	Anton Paar Lovis 2000M/ME	Less than 0.5 %
Conductivity	Radiometer MeterLab CDM 230	1 %

120

121 Density measurements were conducted using a vibrating-tube densimeter DMA 5000 M (Anton  
 122 Paar) in the temperature range from 293.15 to 333.15 K. The apparatus was calibrated using the  
 123 extended calibration procedure with dry air and degassed ultra-pure water (Elga, Veolia) with  
 124 an electrolytic conductivity equals 0.055 $\mu$ S cm<sup>-1</sup> at 298.15 K. With regard to the viscosity-  
 125 related errors, an automatic correction was done using the instrument by measuring the damping  
 126 effect of the sample followed by a mathematical correction of the density. These measurements  
 127 were performed with an uncertainty of less than  $\pm 0.05$  kg m<sup>-3</sup>, whereas repeatability is estimated  
 128 to be  $\pm 0.005$  kg m<sup>-3</sup>. Temperature was measured with an uncertainty of  $\pm 0.02$  K and a resolution  
 129 of  $\pm 0.001$  K.

130 The kinematic viscosity,  $\nu$ , of the investigated systems was determined with a calibrated and  
 131 thermostated rolling-ball viscometer (Lovis 2000 M, Anton Paar), which measures the rolling  
 132 time of a ball through transparent and opaque liquids according to Hoeppler's falling-ball  
 133 principle. The microviscometer is equipped with three calibrated glass capillaries of different  
 134 diameter (1.59, 1.8 and 2.5) mm and steel balls. The dynamic viscosity,  $\eta$ , is obtained by  
 135 measuring the time taken by the steel ball to fall from one side to the end of the capillary filled  
 136 with the sample at a certain angle and temperature, and by knowing the density of the sample.  
 137 The calibration of the capillaries was done using viscosity standards provided by the  
 138 manufacturer and with water. The viscosity was measured with accuracy better than  $\pm 0.5\%$   
 139 (with the same ball and depending on the size of the capillary and the temperature). The  
 140 viscosities were conducted in the temperature range from 293.15 to 333.15 K, and the accuracy  
 141 of the temperature measurements was  $\pm 0.02$  K.

142 The ionic conductivity,  $s$ , was measured using a CDM 230 Conductivity Meter from  
 143 MeterLab<sup>TM</sup>, Radiometer analytical operating at five different frequencies (94 Hz, 375Hz,  
 144 2.93kHz, 23.4kHz and 46.9kHz, depending of the conductance range) with an estimated  
 145 uncertainty of 1%. The conductivity cell was a Radiometer Analytical CDC741T-6 with  
 146 temperature sensor (2-pole Pt sensor,  $K=1.0$  cm<sup>-1</sup>, glass body). Temperature and data

147 acquisitions were made by a personal computer connected to the conductivity meter. The  
148 experimental cell was calibrated with standard 0,1 mol.L<sup>-1</sup> KCl solution, and the resulting cell  
149 constant was 1.0358 cm<sup>-1</sup>. The temperature of the samples was controlled using cryothermostat  
150 polystat with thermal stability  $\pm$  0.03 K. The sample was allowed to spend about 20 min at  
151 constant temperature before performing any single measurement, while 40 min at the phase  
152 transition.

153 All the electrochemical measurements were performed with a three-electrode cell using a  
154 GAMRY REF600 potentiostat. A home-made gold microelectrode of 200  $\mu$ m in diameter was  
155 used as working electrode and a platinum grid of 1x1 cm<sup>2</sup> was used as counter electrode. The  
156 reference electrode was based on the Ag<sup>+</sup> / Ag electrode in a double junction compartment. It  
157 consists of a silver wire immersed in a first junction containing a saturated solution of silver  
158 nitrate (AgNO<sub>3</sub>) in DES, with a sintered glass at the bottom. A second junction containing pure  
159 DES was used to prevent the working solution in the main electrochemical compartment from  
160 any contamination of ions (Ag<sup>+</sup> and NO<sub>3</sub><sup>-</sup>) coming from the first junction containing the  
161 reference electrode. Before each experiment, the working electrode was carefully cleaned by  
162 mechanical grinding with a SiC paper (P4000) followed by an electrochemical cycling in a 0.1  
163 mol L<sup>-1</sup> sulfuric acid aqueous solution by sweeping the potential between -1 and 1.3 V/SCE at  
164 100 mV.s<sup>-1</sup> for 10 min.

165 All the electrochemical experiments were performed under a dry argon atmosphere to avoid the  
166 presence of oxygen and air humidity. All experiments were performed three times.

167

### 168 **3. Results and discussions**

#### 169 *3.1 Physicochemical properties*

170 Variations of the density, viscosity and conductivity of the menthol-based DES and ethaline  
171 were plotted as a function of temperature (in the range 293K - 333K) at atmospheric pressure  
172 on Fig. 3. The temperature dependence of these properties was gathered in Table 2 for menthol-  
173 based DES. As shown on Fig. 3, the density, viscosity and conductivity values of ethaline are  
174 close to some of those reported in the literature [16-21]. For a better comparison, the values  
175 (from this study and from the literature) of the physicochemical parameters of ethaline have  
176 been presented in Table S1. As previously mentioned by some previous work [18, 22], a  
177 disparity in the thermophysical properties of DES exists by comparing the different values even  
178 from a same group of researchers. This discrepancy can be due to the operating conditions or  
179 the water content into the mixtures.

180

181 **Table 2.** Values of some physicochemical parameters of EMIMTFSI at different temperatures at  
 182 pressure ( $p= 0.1$  MPa)

T (K)	density ( $\rho$ in g.cm <sup>-3</sup> )	viscosity ( $\eta$ in mPa.s)	conductivity ( $\sigma$ in mS.cm <sup>-1</sup> )
293.15	1.049065	211.70	0.545
298.15	1.045406	145.82	0.688
303.15	1.041785	103.64	0.854
308.15	1.038154	75.93	1.023
313.15	1.034511	57.13	1.215
318.15	1.030862	43.83	1.430
323.15	1.027218	34.41	1.657
328.15	1.023572	27.56	1.885
333.15	1.019928	22.44	2.180

183

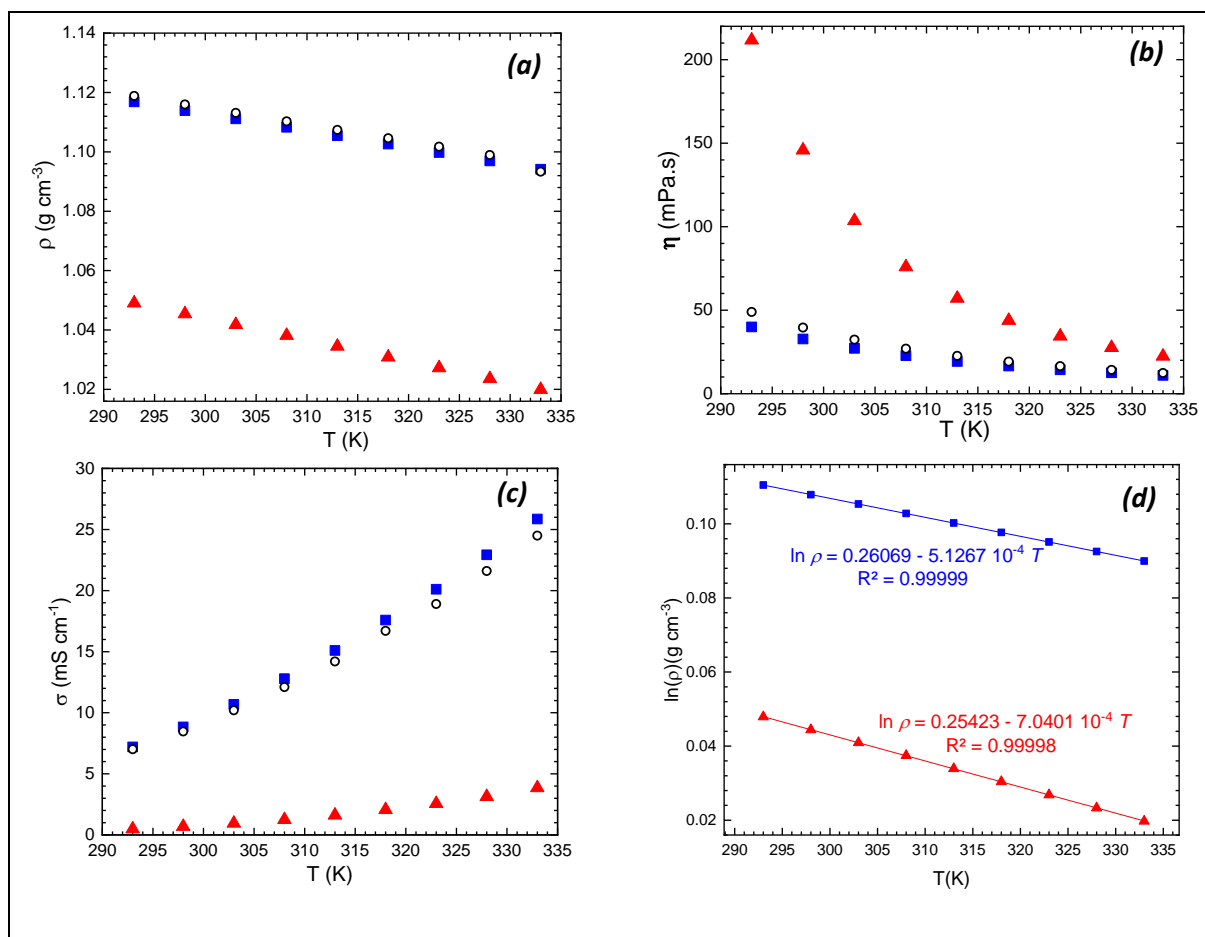
184 The density of both DESs decreases linearly when the temperature increases (Fig3.a), due to  
 185 the molar volume increase leading to a decrease in the average distance between the molecules  
 186 [23]. From the density measurements, the thermal-expansion coefficient,  $\alpha$ , can be calculated  
 187 according to

$$\alpha = \frac{1}{V} \left( \frac{\partial V}{\partial T} \right)_p = -\frac{1}{\rho} \left( \frac{\partial \rho}{\partial T} \right)_p \quad (1)$$

188 Where  $V$  is the molar volume of the DES and  $T$ , the temperature. This thermal expansion  
 189 coefficient is related to the change in volume of the medium with the temperature as shown in  
 190 Eq. 1, and can be linked to the free volume in the solvent. The higher the thermal expansion  
 191 coefficient, the higher the free volume. To determine these thermal expansion coefficients, the  
 192 logarithm of the density ( $\ln \rho$ ) was plotted against the temperature. A straight-line was obtained  
 193 for the both DESs as shown on Fig. 3d. The slope corresponds to the thermal expansion  
 194 coefficient. Table 3 gives the coefficients of thermal expansion of both DESs which were  
 195 compared to the values of a common hydrophobic IL (EMIMTFSI) [24]. Similarly to  
 196 imidazolium based ionic liquids, both DESs are less compressible than common organic  
 197 solvents [25, 26] as toluene ( $11.29 \cdot 10^{-4} \text{ K}^{-1}$  at 298.15K), dichloromethane ( $13.5 \cdot 10^{-4} \text{ K}^{-1}$  at  
 198 298.15K) or ethanol ( $10.9 \cdot 10^{-4} \text{ K}^{-1}$  at 298.15K).



199 It can also be noticed that the thermal expansion coefficient value of the ternary mixture based  
 200 on menthol is lower than the one for the binary menthol – acetic acid studied by Ribiero et al.  
 201 [14] ( $7 \cdot 10^{-4} \text{ K}^{-1}$  for this work compared to  $9.1 \cdot 10^{-4} \text{ K}^{-1}$  for the binary mixture). The addition of  
 202 ethanolamine to the menthol based-DES decreases the free volume thus leading to a less  
 203 compressible solvent.



204 **Figure 3.** Variations of (a) the density, (b) the viscosity, (c) the conductivity and (d) the logarithm of  
 205 the density as a function of the temperature of the DESs - ethaline (blue squares); ethaline from ref.  
 206 [18] (black circles); and DES-Menthol (red triangles).

207  
 208 The dynamic viscosity,  $\eta$ , defines the internal resistance of a fluid to a shear stress. The  
 209 knowledge of its value is of interest for electrochemical applications due to its strong effect on  
 210 the mass transport properties in the solution that significantly affects the diffusion of  
 211 electroactive species in the media. The variations of the DES viscosity as a function of the  
 212 temperature are reported in Fig. 3b. This viscosity profile is similar to what is usually observed  
 213 in the literature for DES mixtures [7, 27, 28], with a more or less marked exponential decrease  
 214 of the viscosity with the increase of the temperature. In a DES, the viscosity is mainly related  
 215 to the formation of hydrogen bonds and van der Waals interactions. Menthol-based DES

216 exhibits higher viscosity than ethaline. For example, at 298 K, the viscosity of menthol-based  
 217 DES is 145 mPa.s, that is, about four times larger than viscosity of ethaline (33 mPa.s) at the  
 218 same temperature. Such a high viscosity for menthol-based DES may be ascribed to the  
 219 presence of a strong hydrogen-bond network between all the components.

220 The temperature dependence of the viscosity values is most often fitted using an Arrhenius-like  
 221 relationship, which expresses as

222

$$\ln \eta = \ln \eta^\infty + \frac{E_\eta}{RT} \quad (2)$$

223 Where  $E_\eta$  is the activation energy,  $\eta$  the viscosity,  $\eta^\infty$  the pre-exponential factor and R the  
 224 perfect gas constant.  $E_\eta$  is the energy barrier that must be overcome by the ions to move through  
 225 the medium. The larger  $E_\eta$ , the harder for the ions to move in the liquid. This equation is based  
 226 on the empirical relationship of Arrhenius for the temperature dependence of reaction rates.  
 227 Most of the time, Eq.2 can be applied to describe the temperature dependence of the viscosity  
 228 in a narrow temperature range. For larger temperature range, another empirical approach the  
 229 so-called Vogel-Tamman-Fulcher (VTF) relationship is commonly used to describe this  
 230 temperature dependence [29]. In parallel, in order to give a better understanding of the viscous  
 231 flow with a thermodynamic light, many authors rely on the Eyring's transition state theory  
 232 applied to the viscosity [30]. In this approach, the viscosity of a liquid is given by

$$\eta = \frac{h\mathcal{N}_a}{V} \exp\left(\frac{\Delta G^\ddagger}{RT}\right) \quad (3)$$

233 where  $\Delta G^\ddagger$  is the molar Gibbs free energy of activation of the viscous flow,  $h$  the Planck's  
 234 constant,  $\mathcal{N}_a$  the Avogadro's number and  $V$  the molar volume of the liquid, which can be  
 235 expressed as,

$$V = \frac{M}{\rho} \quad (4)$$

236 with  $\rho$  the density of the considered DES and  $M$  its molar mass.

237 From Eq. 3 the following expanded relation is obtained

$$\ln \eta = \ln\left(\frac{h\rho\mathcal{N}_a}{M}\right) - \frac{\Delta S^\ddagger}{R} + \frac{\Delta H^\ddagger}{RT} \quad (5)$$

238

239 Where  $\Delta H^\ddagger$  and  $\Delta S^\ddagger$  are the enthalpy and entropy of activation, respectively. By comparison  
 240 of Eq. 2 and Eq. 5, it comes

$$\eta^\infty = \frac{h\rho N_a}{M} \exp\left(-\frac{\Delta S^\ddagger}{R}\right) \quad (6)$$

241 and

$$E_\eta \approx \Delta H^\ddagger \quad (7)$$

242 Eq. 6 shows why some authors introduce the pre-exponential factor of the Arrhenius-like  
 243 relation as an entropic term. This also shows that Eq. 2 can be modelled by a straight-line only  
 244 for narrow temperature range, which widely depends on the variation of the density with the  
 245 temperature. Thus,  $E_\eta = \Delta H^\ddagger$  only if the density can be considered as constant in the  
 246 investigated temperature range. Nevertheless, by plotting  $\ln\left(\frac{M\eta}{h\rho N_a}\right)$  as a function of  $T^{-1}$  for the  
 247 studied DES,  $\Delta H^\ddagger$  and  $\Delta S^\ddagger$  were determined and presented in Table 3, with the value of  $E_\eta$   
 248 determined from Eq. 2. As expected, the activation energy is very close to the enthalpy of  
 249 activation. Moreover, the values of activation entropy are of interest. As shown in Table 3,  
 250 DES-menthol has the highest activation entropy when compared to both ethaline and  
 251 EMIMTFSI: indeed, DES-menthol contains the larger number of compounds.

252

253 **Table 3.** Characteristic parameters for density, viscosity and conductivity variations of the DESs and  
 254 EMIMTFSI determined from their variations as a function of the temperature

Medium	M (/g mol <sup>-1</sup> )	$\alpha$ (/10 <sup>-4</sup> K <sup>-1</sup> )	$E_\eta$ (/kJ mol <sup>-1</sup> )	$E_\sigma$ (/kJ mol <sup>-1</sup> )	$\Delta H^\ddagger$ (/kJ mol <sup>-1</sup> )	$\Delta S^\ddagger$ (/J K <sup>-1</sup> mol <sup>-1</sup> )
Ethaline	87.7	5.1	26.2	25.9	25.8	13.6
DES-Menthol	74.1	7.0	45.4	41.6	44.8	66.0
EMIMTFSI*	391.3	6.6	23.4	20.8	22.8	-5.5

255 \*from ref [24]

256

257 Fig. 3c shows that the conductivity of both DESs increases almost linearly with the temperature.  
 258 This is a direct consequence of a faster movement of ions in the media at higher temperatures.  
 259 At room temperature, the conductivity of ethaline is about 8.8 mS.cm<sup>-1</sup>, which is more than one  
 260 order of magnitude higher than the conductivity measured for the menthol-based DES (0.7  
 261 mS.cm<sup>-1</sup>). Such a difference may be ascribed, at least partially, to the higher viscosity of the

262 menthol-based DES. The conductivity of an ion,  $\sigma_i$ , is linked to its diffusion coefficient,  $D_i$ , as  
 263 expressed by the Nernst-Einstein equation,

$$\sigma_i = \frac{c_i z_i^2 \mathcal{F}^2 D_i}{RT} \quad (8)$$

264 where  $c_i$  stands for the concentration of the ion  $i$  and  $z_i$  its charge. Usually, the diffusion  
 265 coefficient is linked to the viscosity by the Stokes-Einstein relation, defined for a model  
 266 spherical species  $i$  of an effective radius  $r_i$ , as

$$D_i = \frac{k_B T}{6\pi r_i \eta} \quad (9)$$

267 This relation is commonly used to determine the diffusion coefficient of species in IL. However,  
 268 this latter equation is only valid if the ion  $i$  is bigger than the species constituting the medium,  
 269 but there are other relations linking the diffusion coefficient to the reverse of the viscosity taking  
 270 into account, for example, the different characteristic lengths between the species [31].  
 271 Anyhow, we have to keep in mind that the diffusion coefficient is inversely proportional to the  
 272 viscosity. By taking account Eqs. 8 and 9, the conductivity of an ion can be expressed as

$$\sigma_i = \frac{c_i z_i^2 \mathcal{F}^2}{6\pi \mathcal{N}_a r_i \eta} \quad (10)$$

273 The conductivity of the mixtures is the sum of ionic conductivities of the anion and the cation.

$$\sigma = \sigma_{anion} + \sigma_{cation} = \frac{\mathcal{F}^2}{6\pi \mathcal{N}_a \eta} \left( \frac{c_{anion} z_{anion}^2}{r_{anion}} + \frac{c_{cation} z_{cation}^2}{r_{cation}} \right) \quad (11)$$

274 In our case,  $c_{anion} = c_{cation} = c_{salt}$ , then

$$\sigma = \frac{\mathcal{F}^2}{6\pi \mathcal{N}_a \eta} \frac{x_{salt}}{M} \rho \left( \frac{1}{r_{anion}} + \frac{1}{r_{cation}} \right) \quad (12)$$

275  $x_{salt}$  is the molar fraction of the salt in the mixture, ( $x_{salt} = 1$ , for neat IL). Combining Eq. 12 with  
 276 Eq. 2, an Arrhenius-like relationship is obtained

$$\ln \sigma = \ln \sigma^\infty - \frac{E_\sigma}{RT} \quad (13)$$

277 Where  $\sigma^\infty$  is a constant and  $E_\sigma$  is the activation energy for ionic conductivity.  $E_\sigma$  of the DESs  
 278 and EMIMTFSI determined from the experimental data using Eq. 13 are shown in Table 2.

279 By considering, Eqs. 5 and 13, the following expression is then obtained

$$\ln \sigma = \ln \left( \frac{F^2 x_{salt}}{6\pi N_a^2 h} \left( \frac{1}{r_{anion}} + \frac{1}{r_{cation}} \right) \right) + \frac{\Delta S^\ddagger}{R} - \frac{\Delta H^\ddagger}{RT} \quad (14)$$

280

281 Knowing the activation entropy and enthalpy, only the sum  $\left( \frac{1}{r_{anion}} + \frac{1}{r_{cation}} \right)$  can be calculated.

282 As shown in table 3, this value decreases as the temperature increases.

283

284 **Table 3.** Variation of the sum  $\left( \frac{1}{r_{anion}} + \frac{1}{r_{cation}} \right)$  as a function of the temperature

Temperature (/K)	ethaline $\sum_i \frac{1}{r_i}$ (/m)	DES-Menthol $\sum_i \frac{1}{r_i}$ (/m)	EMIMTFSI* $\sum_i \frac{1}{r_i}$ (/m)
293	9.07 10 <sup>9</sup>	3.23 10 <sup>9</sup>	5.32 10 <sup>9</sup>
298	8.30 10 <sup>9</sup>	3.00 10 <sup>9</sup>	5.44 10 <sup>9</sup>
303	7.61 10 <sup>9</sup>	2.76 10 <sup>9</sup>	5.49 10 <sup>9</sup>
308	7.02 10 <sup>9</sup>	2.48 10 <sup>9</sup>	5.44 10 <sup>9</sup>
313	6.47 10 <sup>9</sup>	2.23 10 <sup>9</sup>	5.35 10 <sup>9</sup>
318	5.96 10 <sup>9</sup>	2.00 10 <sup>9</sup>	5.23 10 <sup>9</sup>
323	5.44 10 <sup>9</sup>	1.78 10 <sup>9</sup>	5.09 10 <sup>9</sup>
328	5.01 10 <sup>9</sup>	1.57 10 <sup>9</sup>	4.96 10 <sup>9</sup>
333	4.60 10 <sup>9</sup>	1.42 10 <sup>9</sup>	4.93 10 <sup>9</sup>

285

\*from ref [24]

286

287 For these three media the ions are different as well as their environment. At this stage, the  
 288 analysis of these data is difficult. Indeed, first, it is necessary to check that the hypothesis of  
 289 Stokes-Einstein concerning the size of the ions is always valid. Afterwards, we need an  
 290 assumption or other analysis or calculation to differentiate the anion from the cation. For  
 291 EMIMTFSI, the cation radius can be evaluated by taking the anion radius available in the  
 292 literature [32, 33],  $r_{TFSI} = 3.65 \text{ \AA}$ . Thus, at 298K, the radius of the cation EMIM is around 3.7  
 293  $\text{\AA}$ . For DES, to our knowledge, there is no value for ionic radius, since the environment is very  
 294 different, we chose to only calculate an average radius at 298K to compare these two different  
 295 mixtures. At 298 K, the average radius is about 2.4  $\text{\AA}$  in ethaline and 6.7  $\text{\AA}$  in menthol-based  
 296 DES.

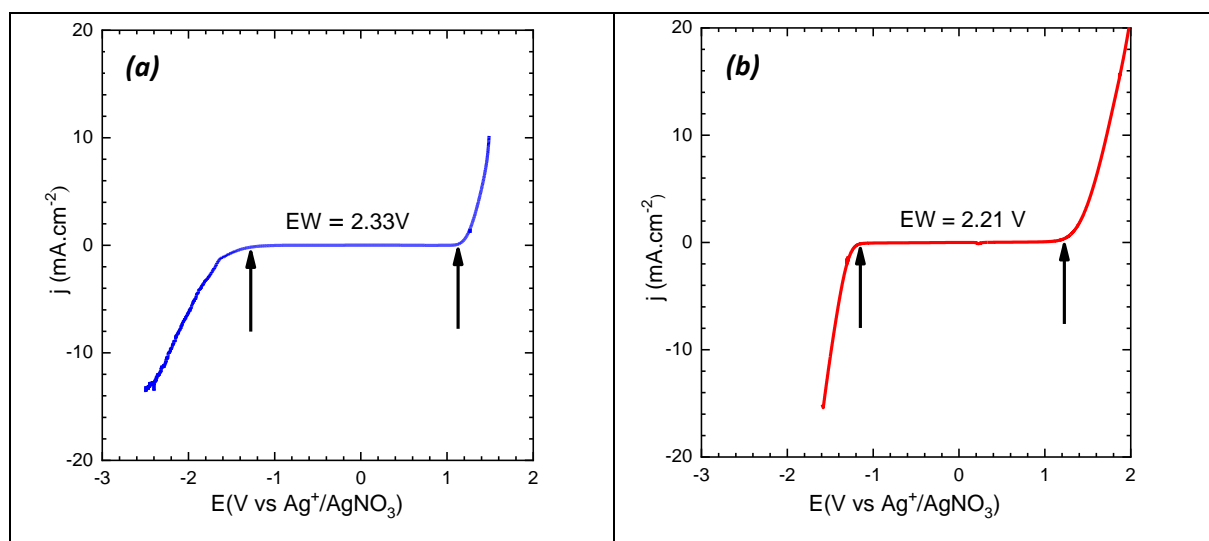
297

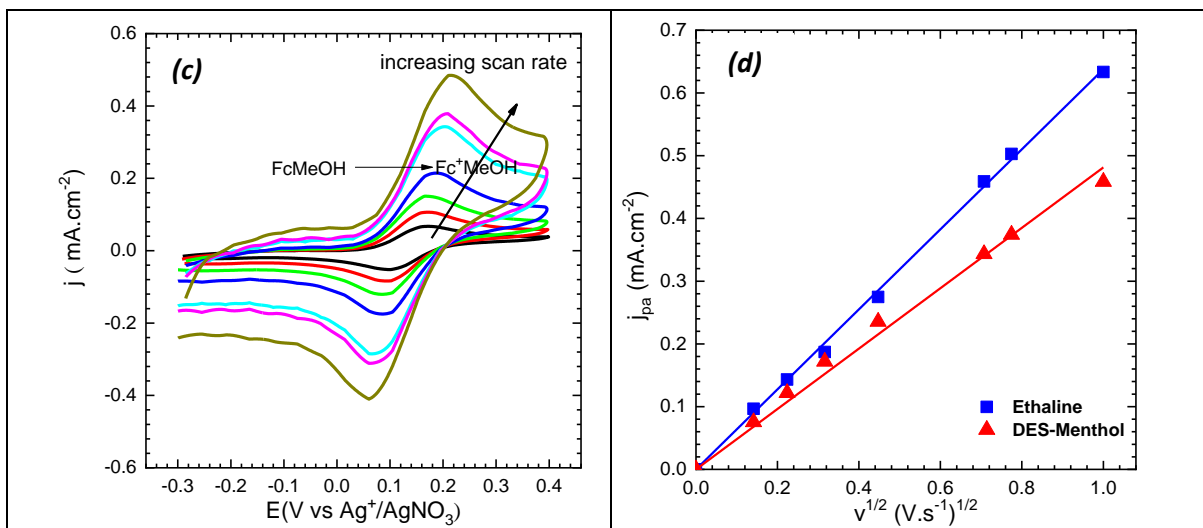
### 298 3.2 Electrochemical properties

299 Before envisioning any practical electrochemical application, it is of interest to determine the  
300 electrochemical window (EW) of the solvents. Figs. 4a and b show the EW of each DES  
301 measured using linear sweep voltammetry (LSV) from -2.5 to 2 V/ $\text{Ag}^+/\text{AgNO}_3$  using a 200  $\mu\text{m}$   
302 in diameter gold electrode. Unlike aprotic ionic liquids, which usually have broad  
303 electrochemical windows spreading over 4 to 5 V [34], the DESs studied in this work display a  
304 lower electrochemical stability comprised in the range 2 to 2.5 V (taking a cutoff value for the  
305 current density of  $\pm 100 \mu\text{A cm}^{-2}$ ). However, this EW is twice larger than the EW of water  
306 electrolyte, which makes these DESs attractive for electrochemical applications.

307 The electrochemical behavior of an electroactive species, the hydroxymethylferrocene  
308 (FcMeOH), in DESs was then studied by cyclic voltammetry (CV) by varying the scan rates  
309 (Fig. 4c). CVs clearly exhibit a quasi-reversible behavior, in which the ratio between the current  
310 density of the anodic peak  $j_{pa}$  and that of the cathodic peak  $j_{pc}$  is close to 1 also at low scan rates  
311 whereas the difference between the anodic and cathodic peak potentials is in agreement with  
312 the predicted values ( $E_{pa} - E_{pc} \approx 60 \text{ mV}$ ) for a mass-transfer controlled system [35]. The current  
313 density peak ( $j_{p1}$ ) varies linearly with the square root of the scan rate (Fig. 4d) showing that the  
314 mass transfer of FcMeOH in the investigated DESs is controlled by the diffusion of  
315 electroactive species [35].

316





317 **Figure 4.** LSV of (a) ethaline and (b) DES-Menthol at a scan rate of  $5\text{mVs}^{-1}$ ; (c) CV of a  $5\text{mM}$   
 318  $\text{FcMeOH}$  in menthol-based DES at different scan rates (from  $20$  to  $1000\text{mVs}^{-1}$ ); (d) variation of the  
 319 current density peak  $j_{pa}$  with the square root of the scan rate for the  $\text{FcMeOH}$  oxidation in DES. All  
 320 these experiments were performed, at  $(25 \pm 0.1)^\circ\text{C}$ , with a gold working electrode ( $200 \mu\text{m}$  in  
 321 diameter).

322  
 323 On this scan rate domain, the diffusion coefficient of  $\text{FcMeOH}$  can thus be obtained from the  
 324 slope of the current intensity curve as a function of square root of sweep rate by using Randles-  
 325 Sevcik equation

$$i_p = 0.446nF \sqrt{\frac{nFv}{RT}} C_i A \sqrt{D_i} \quad (15)$$

326 where  $i_p$  is the current of the peak,  $n$  the number of electron exchanged,  $A$  the electrode surface  
 327 area,  $F$  the Faraday constant,  $D_i$  the diffusion coefficient,  $C_i$  the concentration of the  
 328 electroactive species  $i$ , and  $v$  the scan rate.

329  
 330 **Table 4** Variation of the diffusion coefficient of ferrocene methanol as a function of the viscosity of the  
 331 medium

Medium @298K	$\eta$ (/mPa.s)	$D$ (/ $10^{-7}\text{cm}^2.\text{s}^{-1}$ )
EMIMTFSI*	30.4	3.5
Ethaline	32.7	2.2
DES-Menthol	146	1.1

\*from ref [24]

337 The diffusion coefficients values of FcMeOH in DESs are presented in Table 3. It should be  
338 noticed that the diffusion coefficients obtained in DESs are of the same order of magnitude than  
339 those obtained in the pure ionic liquid (*e.g.* EMIMTFSI). In ethaline the diffusion coefficient  
340 of FcMeOH is twice than in the menthol-based DES. Indeed, as shown in Table 4, ethaline has  
341 a lower viscosity, which explains the more efficient mass transport corresponding to higher  
342 value of the diffusion coefficient. Interestingly, the diffusion coefficient of FcMeOH is of the  
343 same order of magnitude in the DESs and IL studied in this work, showing the great potentials  
344 of the new menthol-based DESs.

345

#### 346 **4. Conclusions**

347 Two deep eutectic solvents (DESs), ethaline and menthol-based DES, have been prepared and  
348 characterized. Hydrophobicity test was performed to show the role of menthol in the mixture.  
349 The addition of ethanolamine to the menthol – acetic acid mixture leads to an increase of the  
350 conductivity. Their physicochemical properties including density, viscosity and conductivity  
351 were studied in detail at different temperatures. Although these mixtures are no conventional,  
352 we estimated an average radius of the ions assuming that the Stokes-Einstein relationship can  
353 be applied.

354 LSV curves at low scan rate allowed obtaining the electrochemical window of DESs. The  
355 electrochemical windows of the two DESs do not show significant differences and are about  
356 2.4 V. The redox couple FcMeOH<sup>+</sup>/FcMeOH is reversible in menthol-based DES and the  
357 diffusion coefficient of FcMeOH is of the same order of magnitude as that obtained in the pure  
358 ionic liquid (EMIMTFSI), thus showing than this DES is suited for performing electrochemical  
359 experiments.

360 Menthol-based DESs are thus a good alternative to hydrophobic ionic liquid for electrochemical  
361 applications (*e.g.* for battery application) especially since it is a biocompatible solvent, easy to  
362 synthesize and cheap.

363

364

#### 365 **Acknowledgements**

366 This work was supported by the Ecole Doctorale Chimie Physique et Chimie Analytique de  
367 Paris Centre (ED 388).

368



369 **References**

- 370 [1] M. Armand, F. Endres, D.R. MacFarlane, H. Ohno, B. Scrosati, Ionic-liquid materials for the  
371 electrochemical challenges of the future, *Nat Mater* 8 (2009) 621-629.
- 372 [2] V.L. Martins, R.M. Torresi, Ionic liquids in electrochemical energy storage, *Curr. Opin. Electrochem.*  
373 9 (2018) 26-32.
- 374 [3] Y. Hu, Z. Wang, X. Huang, L. Chen, Physical and electrochemical properties of new binary room-  
375 temperature molten salt electrolyte based on LiBETI and acetamide, *Solid State Ionics* 175 (2004) 277-  
376 280.
- 377 [4] S.B. Capelo, T. Mendez-Morales, J. Carrete, E. Lopez Lago, J. Vila, O. Cabeza, J.R. Rodriguez, M.  
378 Turmine, L.M. Varela, Effect of temperature and cationic chain length on the physical properties of  
379 ammonium nitrate-based protic ionic liquids, *J. Phys. Chem. B* 116 (2012) 11302-11312.
- 380 [5] E.L. Smith, A.P. Abbott, K.S. Ryder, Deep eutectic solvents (DESs) and their applications, *Chem. Rev.*  
381 114 (2014) 11060-11082.
- 382 [6] C.J. Clarke, W.C. Tu, O. Levers, A. Brohl, J.P. Hallett, Green and Sustainable Solvents in Chemical  
383 Processes, *Chem. Rev.* 118 (2018) 747-800.
- 384 [7] M.A. Kareem, F.S. Mjalli, M.A. Hashim, I.M. AlNashef, Phosphonium-Based Ionic Liquids Analogues  
385 and Their Physical Properties, *J. Chem. Eng. Data* 55 (2010) 4632-4637.
- 386 [8] A.P. Abbott, G. Capper, D.L. Davies, R.K. Rasheed, V. Tambyrajah, Novel solvent properties of  
387 choline chloride/urea mixtures, *Chem Commun (Camb)* (2003) 70-71.
- 388 [9] A.P. Abbott, D. Boothby, G. Capper, D.L. Davies, R.K. Rasheed, Deep eutectic solvents formed  
389 between choline chloride and carboxylic acids: Versatile alternatives to ionic liquids, *J. Am. Chem. Soc.*  
390 126 (2004) 9142-9147.
- 391 [10] C. Teja, F.R. Nawaz Khan, Choline Chloride-Based Deep Eutectic Systems in Sequential Friedlander  
392 Reaction and Palladium-Catalyzed sp(3) CH Functionalization of Methyl Ketones, *ACS Omega* 4 (2019)  
393 8046-8055.
- 394 [11] A. Yadav, S. Pandey, Densities and Viscosities of (Choline Chloride + Urea) Deep Eutectic Solvent  
395 and Its Aqueous Mixtures in the Temperature Range 293.15 K to 363.15 K, *J. Chem. Eng. Data* 59 (2014)  
396 2221-2229.
- 397 [12] Q.H. Zhang, K.D. Vigier, S. Royer, F. Jerome, Deep eutectic solvents: syntheses, properties and  
398 applications, *Chemical Society Reviews* 41 (2012) 7108-7146.
- 399 [13] C. Florindo, L.C. Branco, I.M. Marrucho, Development of hydrophobic deep eutectic solvents for  
400 extraction of pesticides from aqueous environments, *Fluid Phase Equilib.* 448 (2017) 135-142.
- 401 [14] B.D. Ribeiro, C. Florindo, L.C. Iff, M.A.Z. Coelho, I.M. Marrucho, Menthol-based Eutectic Mixtures:  
402 Hydrophobic Low Viscosity Solvents, *ACS Sustainable Chemistry & Engineering* 3 (2015) 2469-2477.
- 403 [15] P. Bonhote, A.P. Dias, M. Armand, N. Papageorgiou, K. Kalyanasundaram, M. Gratzel, Hydrophobic,  
404 highly conductive ambient-temperature molten salts (vol 35, pg 1168, 1996), *Inorg. Chem.* 37 (1996)  
405 166-166.
- 406 [16] A. Yadav, J.R. Kar, M. Verma, S. Naqvi, S. Pandey, Densities of aqueous mixtures of (choline  
407 chloride+ethylene glycol) and (choline chloride+malonic acid) deep eutectic solvents in temperature  
408 range 283.15–363.15K, *Thermochim. Acta* 600 (2015) 95-101.
- 409 [17] A.R. Harifi-Mood, R. Buchner, Density, viscosity, and conductivity of choline chloride + ethylene  
410 glycol as a deep eutectic solvent and its binary mixtures with dimethyl sulfoxide, *J. Mol. Liq.* 225 (2017)  
411 689-695.
- 412 [18] D. Lapeña, L. Lomba, M. Artal, C. Lafuente, B. Giner, Thermophysical characterization of the deep  
413 eutectic solvent choline chloride:ethylene glycol and one of its mixtures with water, *Fluid Phase Equilib.*  
414 492 (2019) 1-9.
- 415 [19] F.S. Mjalli, O.U. Ahmed, Ethaline and Glyceline binary eutectic mixtures: characteristics and  
416 intermolecular interactions, *Asia-Pac. J. Chem. Eng.* 12 (2017) 313-320.
- 417 [20] H. Shekaari, M.T. Zafarani-Moattar, M. Mokhtarpour, S. Faraji, Volumetric and compressibility  
418 properties for aqueous solutions of choline chloride based deep eutectic solvents and Prigogine–Flory–

419 Patterson theory to correlate of excess molar volumes at T = (293.15 to 308.15) K, *J. Mol. Liq.* 289  
420 (2019).

421 [21] H. Shekaari, M. Taghi Zafarani-Moattar, M. Mokhtarpour, S. Faraji, Compatibility of sustainable  
422 solvents ionic liquid, 1-ethyl-3-methylimidazolium ethyl sulfate in some choline chloride based deep  
423 eutectic solvents: thermodynamics study, *J. Chem. Thermodyn.* 141 (2020) 105961.

424 [22] H. Shekaari, M.T. Zafarani-Moattar, M. Mokhtarpour, S. Faraji, Volumetric and compressibility  
425 properties for aqueous solutions of choline chloride based deep eutectic solvents and Prigogine–Flory–  
426 Patterson theory to correlate of excess molar volumes at T = (293.15 to 308.15) K, *J. Mol. Liq.* 289  
427 (2019) 111077.

428 [23] F. Chemat, H. Anjum, A.M. Shariff, P. Kumar, T. Murugesan, Thermal and physical properties of  
429 (Choline chloride + urea +l-arginine) deep eutectic solvents, *J. Mol. Liq.* 218 (2016) 301-308.

430 [24] R. Khalil, N. Chaabene, M. Azar, I.B. Malham, M. Turmine, Effect of the chain lengthening on  
431 transport properties of imidazolium-based ionic liquids, *Fluid Phase Equilib.* 503 (2020) 112316.

432 [25] Z. Gu, J.F. Brennecke, Volume Expansivities and Isothermal Compressibilities of Imidazolium and  
433 Pyridinium-Based Ionic Liquids, *J. Chem. Eng. Data* 47 (2002) 339-345.

434 [26] C. Caleman, P.J. van Maaren, M. Hong, J.S. Hub, L.T. Costa, D. van der Spoel, Force Field Benchmark  
435 of Organic Liquids: Density, Enthalpy of Vaporization, Heat Capacities, Surface Tension, Isothermal  
436 Compressibility, Volumetric Expansion Coefficient, and Dielectric Constant, *J Chem Theory Comput* 8  
437 (2012) 61-74.

438 [27] E.A. Crespo, J.M.L. Costa, A.M. Palma, B. Soares, M.C. Martín, J.J. Segovia, P.J. Carvalho, J.A.P.  
439 Coutinho, Thermodynamic characterization of deep eutectic solvents at high pressures, *Fluid Phase*  
440 *Equilib.* 500 (2019).

441 [28] N.F. Gajardo-Parra, M.J. Lubben, J.M. Winnert, Á. Leiva, J.F. Brennecke, R.I. Canales,  
442 Physicochemical properties of choline chloride-based deep eutectic solvents and excess properties of  
443 their pseudo-binary mixtures with 1-butanol, *J. Chem. Thermodyn.* 133 (2019) 272-284.

444 [29] N.S.M. Vieira, I. Vázquez-Fernández, J.M.M. Araújo, N.V. Plechkova, K.R. Seddon, L.P.N. Rebelo,  
445 A.B. Pereiro, Physicochemical Characterization of Ionic Liquid Binary Mixtures Containing 1-Butyl-3-  
446 methylimidazolium as the Common Cation, *J. Chem. Eng. Data* 64 (2019) 4891-4903.

447 [30] J.F. Kincaid, H. Eyring, A.E. Stearn, The Theory of Absolute Reaction Rates and its Application to  
448 Viscosity and Diffusion in the Liquid State, *Chem. Rev.* 28 (1941) 301-365.

449 [31] H. Eyring, Viscosity, plasticity, and diffusion as examples of absolute reaction rates, *J. Chem. Phys.*  
450 4 (1936) 283-291.

451 [32] G.B. Appetecchi, M. Montanino, D. Zane, M. Carewska, F. Alessandrini, S. Passerini, Effect of the  
452 alkyl group on the synthesis and the electrochemical properties of N-alkyl-N-methyl-pyrrolidinium  
453 bis(trifluoromethanesulfonyl)imide ionic liquids, *Electrochim. Acta* 54 (2009) 1325-1332.

454 [33] H. Shirota, A.M. Funston, J.F. Wishart, E.W. Castner, Jr., Ultrafast dynamics of pyrrolidinium cation  
455 ionic liquids, *J. Chem. Phys.* 122 (2005) 184512.

456 [34] M. Galiński, A. Lewandowski, I. Stępnia, Ionic liquids as electrolytes, *Electrochim. Acta* 51 (2006)  
457 5567-5580.

458 [35] A.J. Bard, L.R. Faulkner, J. Leddy, C.G. Zoski, *Electrochemical methods: fundamentals and*  
459 *applications.* wiley New York, 1980.

460